

## **Analysis of Colour-Magnitude Diagrams of Rich LMC Clusters: NGC 1831**

Basílio X. Santiago, Leandro Kerber, Rodrigo Castro

*Inst. de Física, Univ. Federal do RS, Av. Bento Gonçalves, 9500, Porto Alegre, RS 91501-970, Brazil*

Mark Wilkinson, Richard de Grijs, Rachel Johnson, Gerry Gilmore

*Inst. of Astronomy, Madingley Rd, Cambridge, CB3 0HA, UK*

Sylvie Beaulieu

*University of Victoria, Victoria, B.C., Canada, V8W 3P6*

**Abstract.** We present a preliminary analysis of a deep colour-magnitude diagram of NGC 1831, a rich cluster in the LMC. The data were obtained with HST/WFPC2 in the F555W and F814W filters, reaching  $m_{555} \simeq 25$  mag. Efficient use of the two-dimensional distribution of data was made by comparing the observed colour-magnitude diagram with model ones. We discuss the process used in accounting for field star contamination and sampling incompleteness in the data. We also describe the algorithm used in building artificial diagrams from model isochrones and the statistical method used in comparing model and data colour-magnitude diagrams. From these comparisons we infer a metallicity  $Z = 0.008$  and a low value,  $f_{bin} \simeq 0.25$ , for the global binary fraction of NGC 1831. We also rule out ages  $\tau \lesssim 500$  Myr and mass function slope values  $\alpha \gtrsim 2$ .

### **1. Introduction**

Santiago et al. (2001) have presented luminosity functions (LFs) for 6 rich LMC clusters targeted in the Cycle 7 HST project “Formation and Evolution of Rich LMC Star Clusters” (Beaulieu et al. 1998). Mass segregation was observed in all clusters, as were shape variations in their position-dependent LFs within each cluster. Mass functions (MFs) were also built from the LFs for the 2 youngest members of the sample, NGC 1805 and NGC 1818. This transformation from luminosities into masses, however, is plagued with difficulty: uncertainties in the cluster metallicity and age are incorporated into the transformation, since the mass-luminosity relation depends on age and metallicity (Baraffe et al. 1998; Charbonnel et al. 1999). The mass-luminosity relation itself is often uncertain, especially for low mass and/or low-metallicity stars. Furthermore, unresolved binaries make an inferred LF or MF shallower than the true one.

With these issues in mind, it is better to infer a cluster’s MF simultaneously with its binary fraction, its age and metal abundance. Here we show a first

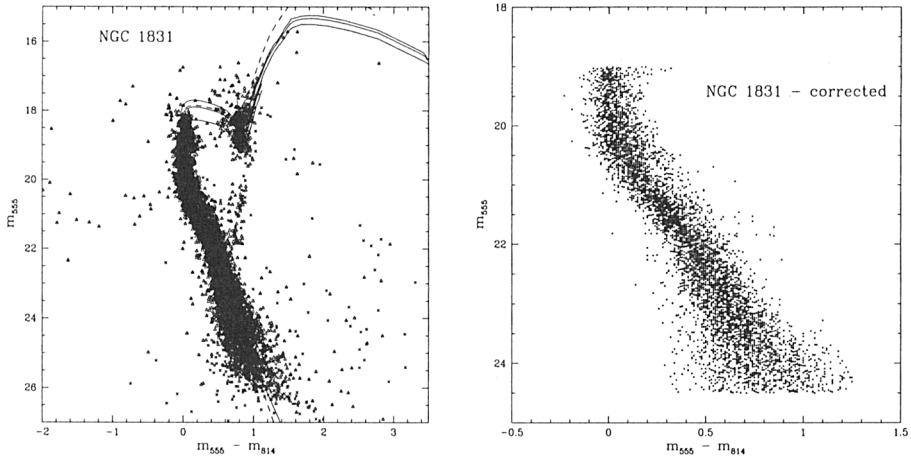


Figure 1. Left panel: cluster and field colour-magnitude diagrams: triangles: stars found in the NGC 1831 cluster image; crosses: stars from off-cluster WFPC2 images. Padova isochrones correspond to ages  $\tau = 400, 500, 600$  Myr and  $Z = 0.008$  (solid lines) and  $\tau = 500$  Myr and  $Z = 0.004$ . Right panel: completeness corrected and field subtracted CMD of NGC 1831.

attempt to do that for NGC 1831, one of the rich LMC clusters in our sample. We model the colour-magnitude diagram (CMD) of NGC 1831, simultaneously inferring its age  $\tau$ , metallicity  $Z$ , mass function slope  $\alpha$  and fraction of unresolved binaries  $f_{bin}$ .

## 2. The colour-magnitude diagram of NGC 1831

HST/WFPC2 images in the filters F555W and F814W were obtained for NGC 1831 as part of the project. The data processing, including calibration, sample selection and photometry is discussed in Santiago et al. (2001). The resulting CMD for the cluster is represented as the triangles in Fig. 1. It shows a well defined main-sequence (MS) and red giant branch (RGB). Superimposed are Padova isochrones (Girardi et al. 2000) which fit the cluster MS and the RGB; the lower part of this latter is dominated by field stars. These latter, taken from a field 7.3' away from NGC 1831 (Castro et al. 2001), are represented in Fig. 1 as crosses.

### 2.1. Completeness effects

The CMD shown in Figure 1 suffers from increasing incompleteness at faint magnitudes. Artificial star experiments were carried out to quantify this loss of stars as a function of magnitude and position within the cluster. They are described in more detail in Santiago et al. (2001). As the model CMDs do not suffer from this effect, we statistically incorporated the missing stars into the

observed CMD. For each observed star, extra points were added to the CMD according to its inverse completeness value. These extra points were randomly spread out from MS fiducial points according to the uncertainties in the colour and magnitude of each generating star. A Gaussian distribution of photometric errors in both V and I bands was assumed when spreading out the extra stars. This procedure for accounting for completeness effects is described in more detail in Kerber et al. (2001b).

## 2.2. Field star subtraction

Stars belonging to the LMC field are also present in the CMD shown in Figure 1. Our model CMDs are created for a single stellar population and as such do not accommodate field stars. We therefore statistically removed these latter with the help of the nearby off-cluster CMD obtained by Castro et al. (2001). For each pair of cluster/off-cluster star (pairs of triangles/crosses in the CMD of Fig 1) we estimated the probability that it could be made up of two independent photometric measurements of the same star. This probability was estimated again considering the photometric uncertainties in both data points and a Gaussian distribution of errors. For each star in the off-cluster field, a cluster star was then randomly eliminated from the CMD, according to the estimated matching probabilities.

Figure 1 (right panel) shows the resulting CMD corrected for completeness and field contamination. Notice that both corrections preserve the shape and mean position of the cluster MS as traced by the stars in the left panel. The data have been cut-off at bright ( $m_{555} < 19$ ) and faint ( $m_{555} > 24.5$ ) ends in order to avoid saturation effects or regions where completeness corrections would dominate the CMD. Foreground stars and background unresolved galaxies were also thrown away by applying cuts below and above the MS.

The turn-off at  $m_{555} \simeq 22$ , identified by Castro et al. (2001) as the old ( $\tau \gtrsim 10$  Gyr) LMC stellar component, has been considerably depleted. Even though some residual stars in this turn-off region remain in the CMD, the statistical subtraction method just outlined yields a cleaner CMD than that of simply eliminating the closest cluster star to each field star. We again refer to Kerber et al. (2001b) for a more detailed discussion.

## 3. The model colour-magnitude diagrams

### 3.1. Input model parameters and algorithm

Artificial CMDs representative of a particular stellar population were generated from a code kindly provided by David Valls-Gabaud and adapted to the present problem by LK. The main input parameters are  $\tau$ ,  $Z$ ,  $\alpha = d \log \phi(m) / d \log m$ , and  $f_{bin}$ , as defined in the Introduction. Stellar masses were randomly selected from the power-law PDMF; their absolute magnitudes in the F555W and F814W filters were then taken from the isochrone corresponding to the population's chosen age and metallicity. We used Padova isochrones from Girardi et al. (2000) and interpolated in  $Z$  when necessary. Given the distance modulus to the LMC, taken to be 18.5 (Panagia et al. 1991), absolute magnitudes were then converted into apparent magnitudes, to which the photometric uncertainties (discussed in

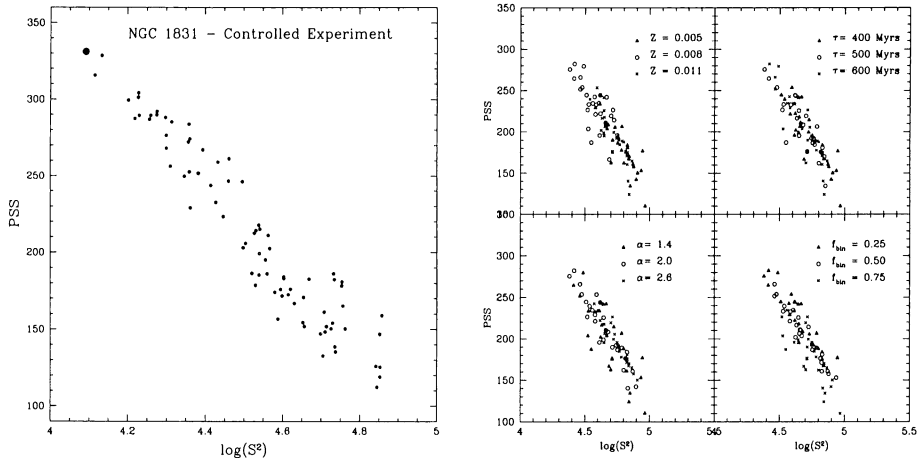


Figure 2. Left panel:  $pss$  vs.  $s^2$  diagram for a controlled experiment where model vs. model CMD comparisons are made; Right panel: same diagram showing the preliminary results for NGC 1831 in a four-panelled version

more detail in Santiago et al. 2001) were added. Finally, a fraction  $f_{bin}$  of the stars were added to a companion, created in the same way, their magnitudes and colour combined in order to simulate the effect of unresolved binarism. The artificial CMDs built this way were also cut in the same way as the observed data in order to compare real and model data within the same CMD region.

### 3.2. The model grid

Our grid of models covers a 4-dimensional parameter space of  $\tau$ ,  $Z$ ,  $\alpha$  and  $f_{bin}$ . The parameter values used were:  $\tau = 400, 500, 600$  Myr;  $Z = 0.005, 0.008, 0.011$ ;  $\alpha = 1.4, 2.0, 2.6$ ;  $f_{bin} = 0.25, 0.50, 0.75$ . Therefore, we created CMDs for 81 different models, each one represented by a point in parameter space.

## 4. Preliminary results and discussion

We compare each artificial CMD in turn to the observed one. For that purpose we use statistical tools that take into account the 2D information in them. We use two simple but objective statistics: a dispersion ( $s^2$ ) and a joint probability that the two CMDs being compared are drawn from the same population ( $pss$ ). These are explained in more detail in Kerber et al. (2001a).

Before applying these statistics to the model vs. data comparison, we tested them on model vs. model comparisons. We took a random realization of one of the 81 models in the grid and compared it to realizations from all the models. Figure 2 (left panel) shows the diagram  $pss$  vs.  $s^2$  for this controlled experiment. Each point in the diagram is the result of comparing one model realization to the randomly chosen one. As desirable and expected, there is a clear correlation

between both statistics in the sense that the larger the value of  $pss$ , the smaller the dispersion  $s^2$ . Another reassuring result from this figure is that the comparison involving two realizations from the same model (large dot) yields the largest (smallest)  $pss$  ( $s^2$ ) value, indicating that we recover the model that best describes “the data”.

In Figure 2 (right panel) we show the  $pss$  vs.  $s^2$  diagram for the NGC 1831 CMD. The same points are shown in all 4 panels but, in each case, the different symbols represent different values along a fixed axis in the model parameter space, as indicated. This allows us to infer the 4 parameter values of any particular model. The best models are again located in the upper left of the diagrams, and clearly correspond to  $Z = 0.008$  (upper left panel). We also infer a low binary fraction,  $f_{bin} = 0.25$  (lower right panel). For the age and PDMF slope we can so far only rule out the lowest and largest grid values, respectively.

**Acknowledgments.** David Valls-Gabaud has greatly helped this work not only by providing part of the programs used in the analysis but also by making very useful comments. We thank Leo Girardi for kindly sending us the Padova evolutionary tracks in appropriate formats. The authors have greatly benefitted from the privilege of working along with the late Becky Elson. This work was partially supported by CNPq and PRONEX/FINEP 76.97.1003.00.

## References

- Baraffe, I., Chabrier, G., Allard, F., Hauschildt, P.H., 1998, *A&A*, 337, 403  
 Beaulieu, S.F. et al. 1998, in *New Views of the Magellanic Clouds*, IAU Symp. 190, eds. Y.-H. Chu, N. Suntzeff, J. Hesser & D. Bohlender (San Francisco: ASP), 460  
 Castro, R., Santiago, B., Gilmore, G., Beaulieu, S., Johnson, R., 2001, *MNRAS*, 326, 333  
 Charbonnel, C., Brown, J., Wallerstein, G., 1999, *A&AS*, 135, 405  
 Girardi, L., Bressan, A., Bertelli, G., Chiosi, C., 2000, *A&AS*, 141, 371  
 Kerber, L.O., Javiel, S.C., Santiago, B.X., 2001a, *A&A*, 365, 424  
 Kerber, L.O., et al., *A&A*, 2001b, in preparation  
 Panagia, N., Gilmozzi, R., Macchetto, F., Adorf, H.-M., Kirshner, R., 1991, *ApJ*, 380, L23  
 Santiago, B., Beaulieu, S., Johnson, R.A., Gilmore, G. 2001, *A&A*, 369, 74

## Discussion

*J. Gallagher:* Have you explored the impact of using different sets of isochrones on your conclusions?

*B. Santiago:* No, not yet. We notice, however, that the Padova isochrones fit the fiducial points we define along the main-sequence very well, at least for the cases of NGC 1831 and NGC 1868.

*G. Piotto:* It would be useful to have the error bars in the plot of the LF slopes against radial distances. A 0.2 units difference in the slopes seems rather small.

*B. Santiago:* Absolutely, I should have put error bars on those plots. The fit quality does vary from panel to panel as one can confirm by just looking at the LFs. As for the LF slope differences, my understanding is that, as  $L \approx M^{3.5}$  or so, a 0.2 difference in LF slope turns into a 0.7 difference in MF slope.